Inorganic Chemistry

Article

pubs.acs.org/IC

Geometric Control of Nuclearity in Copper(I)/Dioxygen Chemistry

Tsukasa Abe,[†] Yuma Morimoto,[†] Tetsuro Tano,[†] Kaoru Mieda,[§] Hideki Sugimoto,[†] Nobutaka Fujieda,[†] Takashi Ogura,[§] and Shinobu Itoh*[,†]

[†]Department of Material and Life Science, Division of Advanced Science and Biotechnology, Graduate School of Engineering, Osaka University, 2-1 Yamadaoka, Suita, Osaka 565-0871, Japan

[§]Picobiology Institute, Graduate School of Life Science, University of Hyogo, RSC-UH LP Center, Koto 1-1-1, Sayo-cho, Sayo-gun, Hyogo 679-5148, Japan

Supporting Information

ABSTRACT: Copper(I) complexes supported by a series of N_3-tridentate ligands bearing a rigid cyclic diamine framework such as 1,5-diazacyclooctane (**L8**, eight-membered ring), 1,4-diazacycloheptane (**L7**, seven-membered ring), or 1,4-diazacyclohexane (**L6**, six-membered ring) with a common 2-(2-pyridyl)ethyl side arm were synthesized and their reactivity toward O_2 were compared. The copper(I) complex of **L8** preferentially provided a mononuclear copper(II) end-on superoxide complex **S** as reported previously [Itoh, S., et al. *J. Am. Chem. Soc.* **2009**, 131, 2788−2789], whereas a copper(I) complex of **L7** gave a bis(μ-oxido)dicopper(III) complex **O** at a low temperature (−85 °C) in acetone. On the other hand, no such active-oxygen complex was detected in the oxygenation reaction of the copper(I) complex of **L6** under the same conditions. In addition, O_2-reactivity of the copper(I) complex supported by an acyclic version of the tridentate ligand (**LA**, $PyCH_2CH_2N(CH_3)CH_2CH_2CH_2N(CH_3)_2$; Py = 2-pyridyl) was examined to obtain a mixture of a (μ−η^2:η^2-peroxido)dicopper(II) complex ^{S}**P** and a bis(μ-oxido)dicopper(III) complex **O**. Careful inspection of the crystal structures of copper(I) and copper(II) complexes and the redox potentials of copper(I) complexes has revealed important geometric effects of the supporting ligands on controlling nuclearity of the generated copper active-oxygen complexes.

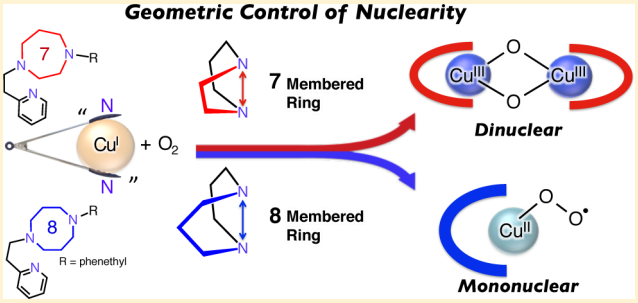

INTRODUCTION

Copper(I)/dioxygen chemistry has long been an important research objective not only in chemistry but also in biology and physiology, since it has strong relevance to the oxidation and oxygenation reactions in biological as well as industrial chemical processes.[1−11] To get insights into the structure, physicochemical properties, and reactivity of the copper active-oxygen species involved in those reactions, a great deal of effort has been made to develop efficient ligands, which enable us to control copper(I)-dioxygen reactivity. So far, several types of copper-dioxygen complexes with different nuclearity (mononuclear, dinuclear, trinuclear, and tetranuclear) have been structurally characterized, and their physicochemical properties and reactivity have been explored in detail.[5,6,12]

In most cases, the reaction of copper(I) complexes and O_2 provides dinuclear copper dioxygen complexes such as end-on and side-on (μ-peroxido)dicopper(II) complexes, ^{E}**P** and ^{S}**P**, and/or bis(μ-oxido)dicopper(III) complex **O**, since initially formed mononuclear copper-dioxygen adduct complexes are easily trapped by another molecule of copper(I) starting complex.[5] Thus, sterically demanding supporting ligands have been usually adopted to prevent such a dimerization reaction for the studies of mononuclear copper-dioxygen adducts.[13−15] Intramolecular hydrogen bonding interaction as well as ligands with strongly electron donating nature such as amide anion or 4-(dimethylamino)pyridine were also employed to stabilize the mononuclear copper(II)-superoxide complexes.[16−18] However, much less attention has been paid to geometric effects of the supporting ligands on the stability of the mononuclear copper-dioxygen adduct complexes, even though biological systems finely tune the reactivity of copper centers with well-positioned amino acid residues.[3]

In this respect, we have recently reported that an N_3-tridenate ligand consisting of 1,5-diazacyclooctane with 2-(2-pyridyl)ethyl side arm (**L8**, Chart 1) provides a mononuclear copper(II) end-on superoxide complex **S** (Scheme 1), the structure (distorted tetrahedron) and reactivity (aliphatic hydroxylation) of which are similar to those of a putative reactive intermediate involved in copper monooxygenases such as peptidylglycine α-hydroxylating monooxygenase (PHM) and dopamine β-monooxygenase (DβM).[19,20] Notably, ligand **L8** has neither sterically bulky substituents nor strongly electron-donating donor groups. Thus, the unique stability of the mononuclear copper(II)-superoxide complex **S** of ligand **L8** may be attributed to a distinctive geometric feature of the

Received: June 19, 2014
Published: August 7, 2014

 © 2014 American Chemical Society dx.doi.org/10.1021/ic501461n | *Inorg. Chem.* 2014, 53, 8786−8794

Chart 1. Ligands L8, L7, L6, and LA

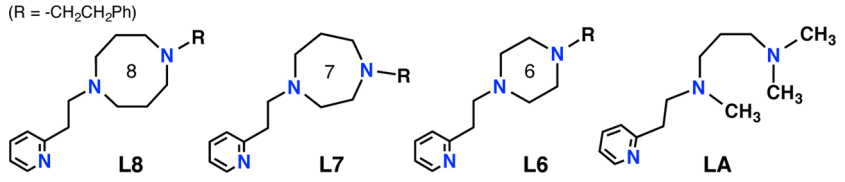

Scheme 1. Copper-Dioxygen Complexes

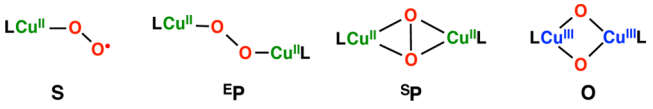

supporting ligand. To address this intriguing issue, we herein examined the oxygenation reaction of the copper(I) complexes supported by similar N_3-tridentate ligands but having smaller cyclic diamine moiety **L7** (seven-membered ring) and **L6** (six-membered ring). In contrast to the case of ligand **L8**, oxygenation reaction of the copper(I) complex of **L7** gave a bis(μ-oxido)dicopper(III) complex **O**, whereas no active-oxygen intermediate was detected during the course of the oxygenation reaction of copper(I) complex of **L6** under the same conditions. In addition, O_2-reactivity of the copper(I) complex supported by an acyclic version of the tridentate ligand **LA** (Chart 1) was examined to find formation of a mixture of a (μ-η^2:η^2-peroxido)dicopper(II) complex ^{S}**P** and a bis(μ-oxido)dicopper(III) complex **O**. Careful inspection of the crystal structures of copper(I) and copper(II) complexes and the redox potentials of copper(I) complexes have revealed important geometric effects of the supporting ligands on controlling nuclearity of the generated copper active-oxygen complexes.

EXPERIMENTAL SECTION

General. The reagents and the solvents used in this study, except the ligands and the copper complexes, were commercial products of the highest available purity and were further purified by the standard methods, if necessary.[21] The ligand 1-(2-phenethyl)-5-[2-(2-pyridyl)-ethyl]-1,5-diazacyclooctane (**L8**) and the corresponding copper(I) complex [Cu^{I}(**L8**)]$^+$ and copper(II) chloride complex [Cu^{II}(**L8**)-(Cl)]$^+$ were synthesized according to the reported procedure.[19,20] FT-IR spectra were recorded on a Jasco FTIR-4100, and UV−visible spectra were taken on a Jasco V-570 or a Hewlett-Packard 8453 photo diode array spectrophotometer equipped with a Unisoku thermostated cryostat cell holder USP-203. ^{1}H NMR spectra were recorded on a JEOL ECS400 spectrometer and a Bruker Avance III HD NMR spectrometer. Mass spectra were recorded on a JEOL JMS-700T Tandem MS-station mass spectrometer. ESI-MS (electrospray ionization mass spectra) measurements were performed on a PerSeptive Biosystems Mariner Biospectrometry workstation. Elemental analyses were performed on a Yanaco New Science Inc. CHN order MT-5 or a J-Science Lab Co., Ltd. Micro Corder JM10. Electrochemical measurements (cyclic voltammetry) were performed at 298 K using Automatic Polarization System HZ-7000 and HZ-3000 Hokutodenko in deaerated acetone containing $TBAPF_6$ (tetrabutylammonium hexafluorophosphate, 0.10 M) as a supporting electrolyte. A conventional three-electrode cell was used with a glassy carbon working electrode and a platinum wire as a counter electrode. The measured potentials were recorded with respect to $Ag/AgNO_3$ (1.0×10^{-2} M). All electrochemical measurements of the copper(I) complexes were carried out under a nitrogen atmosphere. The one-electron oxidation potential values (E_{ox}) (vs $Ag/AgNO_3$) were converted to those vs SCE by adding 0.29 V.[22]

Synthesis. *1-(tert-Butyloxycarbonyl)-4-(2-phenethyl)-1,4-diazacycloheptane.* A CH_3CN-H_2O (50 mL: 30 mL, 80 mL) solution containing 1-(*tert*-butyloxycarbonyl)-1,4-diazacycloheptane (0.99 g, 4.9 mmol),[23] (2-bromoethyl)benzene (2.7 g, 15 mmol), and Na_2CO_3 (2.6 g, 25 mmol) was refluxed for 15 h at 70 °C. Removal of the solvent by evaporation gave brown oil, to which NaOH (aq) was added slowly until the pH of the solution became 14. The aqueous solution was extracted with CH_2Cl_2 (80 mL × 3), and the combined organic layer was dried over Na_2SO_4. After removal of Na_2SO_4 by filtration, evaporation of the solvent gave brown oil, from which the titled compound was isolated as colorless oil in 69% by silica column chromatography (eluent: AcOEt). ^{1}H NMR ($CDCl_3$, 400 MHz) δ 1.46 (9 H, s, $-CH_3$), 1.84 (2 H, pentet, J = 6.8 Hz, $-CH_2-$), 2.68−2.81 (8 H, m, $-CH_2-$), 3.43−3.47 (4 H, m, $-CH_2-$), 7.20−7.27 (5 H, m, Ar*H*); FT-IR (neat) ν 1689 and 1408 cm^{-1} (C═O); HRMS (FAB$^+$) m/z = 305.2237, calcd for $C_{18}H_{29}N_2O_2$ = 305.2229.

1-(2-Phenethyl)-1,4-diazacycloheptane. To a solution of 1-(*tert*-butyloxy-carbonyl)-4-(2-phenethyl)-1,4-diazacycloheptane (1.0 g, 3.4 mmol) in CH_2Cl_2 (34 mL) was added slowly trifluoroacetic acid (1.9 g, 17 mmol) at 0 °C (ice bath). The solution was stirred at this temperature for 15 min and then at ambient temperature for a day. Removal of the solvent by evaporation gave pale yellow oil, to which NaOH (aq) was added slowly until the pH of the solution became about 7. The aqueous solution was extracted with CH_2Cl_2 (30 mL × 3), and the combined organic layer was dried over Na_2SO_4. After removal Na_2SO_4 by filtration, evaporation of the solvent gave pale yellow oil quantitatively. ^{1}H NMR ($CDCl_3$, 400 MHz) δ 1.78 (2 H, pentet, J = 5.8 Hz, $-CH_2-$), 1.86 (1 H, br, $-NH-$), 2.74−2.80 (8 H, m, J = 5.8 Hz, $-CH_2-$), 2.91−2.96 (4 H, m, $-CH_2-$), 7.18−7.28 (5 H, m, Ar*H*); HRMS (FAB$^+$) m/z = 205.1704, calcd for $C_{13}H_{21}N_2$ = 205.1705.

*1-(2-Phenethyl)-4-[2-(2-pyridyl)ethyl]-1,4-diazacycloheptane (**L7**).* A methanol solution (50 mL) containing 1-(2-phenethyl)-1,4-diazacycloheptane (0.51 g, 2.5 mmol), 2-vinylpyridine (1.3 g, 13 mmol), and acetic acid (0.75 g, 13 mmol) was refluxed for 2 days at 60 °C. Removal of the solvent by evaporation gave brown oil, from which ligand **L7** was obtained as pale yellow oil in 60% by alumina column chromatography (eluent: AcOEt/MeOH = 9/1). ^{1}H NMR ($CDCl_3$, 400 MHz) δ 1.83 (2 H, pentet, J = 4.0 Hz, $-CH_2-$), 2.70−2.82 (12 H, m, $-CH_2-$), 2.88−3.00 (4 H, m, $-CH_2-$), 7.08−7.11 (1 H, m, Ar*H*), 7.19 (4 H, m, Ar*H*), 7.29 (2 H, m, Ar*H*), 7.60 (1 H, t, J = 8.0 Hz, PyH_4), 8.52 (1 H, d, J = 4.4 Hz, PyH_6); HRMS (FAB$^+$) m/z = 310.2282, calcd for $C_{20}H_{28}N_3$ = 310.2283.

1-(tert-Butyloxycarbonyl)-4-(2-phenethyl)-1,4-diazacyclohexane. This compound was prepared by the same procedures as described for the synthesis of 1-(*tert*-butyloxycarbonyl)-4-(2-phenethyl)-1,4-diazacycloheptane using 1-(*tert*-butyloxycarbonyl)-1,4-diazacyclohexane[37] instead of 1-(*tert*-butyloxycarbonyl)-1,4-diazacycloheptane in 78%. ^{1}H NMR ($CDCl_3$, 400 MHz) δ 1.46 (9 H, s, $-CH_3$), 2.47 (4 H, t, J = 4.8 Hz, $-CH_2-$), 2.59−2.63 (2 H, m, $-CH_2-$), 2.79−2.83 (2 H, m, $-CH_2-$), 3.47 (4 H, t, J = 5.2 Hz, $-CH_2-$), 7.20 (3 H, m, J = 8.0 Hz, Ar*H*), 7.27−7.31 (2 H, m, J = 8.0 Hz, Ar*H*); FT-IR (KBr) ν 1688 and 1415 cm^{-1} (C═O); HRMS (FAB$^+$) m/z = 291.2066, calcd for $C_{17}H_{27}O_2N_2$ = 291.2073.

1-(2-Phenethyl)-1,4-diazacyclohexane. This compound was prepared by the same procedures as described for the synthesis of 1-(2-phenethyl)-1,4-diazacycloheptane using 1-(*tert*-butyloxycarbonyl)-4-(2-phenethyl)-1,4-diazacyclohexane instead of 1-(*tert*-butyloxycarbonyl)-4-(2-phenethyl)-1,4-diazacycloheptane quantitatively. ^{1}H NMR ($CDCl_3$, 400 MHz) δ 2.50 (4 H, br m, $-CH_2-$), 2.56−2.60 (2 H, m, $-CH_2-$), 2.79−2.83 (2 H, m, $-CH_2-$), 2.91−2.94 (4 H, t, J = 4.8

dx.doi.org/10.1021/ic501461n | Inorg. Chem. 2014, 53, 8786−8794

Hz, $-CH_2-$), 7.17−7.21 (3 H, t, J = 8.0 Hz, ArH), 7.28 (2 H, t, J = 8.0 Hz, ArH); HRMS (FAB$^+$) m/z = 191.1551, calcd for $C_{12}H_{19}N_2$ = 191.1548.

*1-[(2-Phenethyl)]-4-[2-(2-pyridyl)ethyl]-1,4-diazacyclohexane (**L6**).* Ligand **L6** was prepared by the same procedures as described for the synthesis of 1-(2-phenethyl)-4-[2-(2-pyridyl)ethyl]-1,4-diazacycloheptane **L7** using 1-(2-phenethyl)-1,4-diazacyclohexane instead of 1-(2-phenethyl)-1,4-diazacycloheptane in 67%. ^{1}H NMR ($CDCl_3$, 400 MHz) δ 2.59−2.63 (10 H, m, $-CH_2-$), 2.77−2.84 (4 H, m, J = 7.6 Hz, $-CH_2-$), 2.99−3.03 (2 H, m, J = 7.6 Hz, $-CH_2-$), 7.10−7.13 (1 H, m, ArH), 7.21 (4 H, m, ArH), 7.27−7.30 (2 H, m, ArH), 7.60 (1 H, t, J = 6.0 Hz, PyH_4), 8.53 (1 H, d, J = 4.4 Hz, PyH_6); HRMS (FAB$^+$) m/z = 296.2126, calcd for $C_{19}H_{26}N_3$ = 296.2127.

*[Cu^I(**L7**)](PF6).* Ligand **L7** (26 mg, 84 μmol) was treated with an equimolar amount of $[Cu^I(CH_3CN)_4](PF_6)$ (31 mg, 84 μmol) in THF/CH_3CN (2.7 mL/0.30 mL) under N_2 atmosphere in a glovebox (KK-011-AS, Korea Kiyon product). After stirring the mixture for 10 min at ambient temperature, addition of ether (50 mL) to the mixture gave a yellowish green powder that was precipitated by letting the mixture stand for several minutes. The supernatant was then removed by decantation, and the remaining yellowish green solid was washed with ether several times and dried to give complex $[Cu^I(\mathbf{L7})](PF_6)$ in 53%. Single crystals of $[Cu^I(\mathbf{L7})](PF_6)$ were obtained by vapor diffusion of ether into a THF solution of the complex. FT-IR (KBr) ν 841 cm^{-1} (PF_6^-); HRMS (FAB$^+$): m/z = 372.1497, calcd for $C_{20}H_{27}CuN_3$ 372.1501; Anal. Calcd for $[Cu^I(\mathbf{L7})](PF_6)\cdot 0.3H_2O$ ($C_{20}H_{27.7}CuF_6N_3O_{0.3}P_1$): C, 45.85; H, 5.32; N, 8.02. Found: C, 45.94; H, 5.59; N, 7.81.

*[Cu^{II}(**L7**)(Cl)$_2$].* Ligand **L7** (20 mg, 65 μmol) was treated with an equimolar amount of $Cu^{II}Cl_2$ (8.7 mg, 65 μmol) in CH_3CN (3.0 mL). After stirring the mixture for 10 min at ambient temperature, addition of ether (50 mL) to the solution gave a green powder that was precipitated by standing the mixture for several minutes. The supernatant was then removed by decantation, and the remaining green solid was washed with ether three times and dried to give complex $[Cu^{II}(\mathbf{L7})(Cl)_2]$ in 52%. Single crystals of $[Cu^{II}(\mathbf{L7})(Cl)_2]$ were obtained by vapor diffusion of ether into a CH_3CN solution of the complex. HRMS (FAB$^+$): m/z = 407.1188, calcd for $C_{20}H_{27}ClCuN_3$ 407.1190; Anal. Calcd for $[Cu^{II}(\mathbf{L7})(Cl)_2]\cdot 0.5H_2O$ ($C_{20}H_{28}Cl_2CuN_3O_{0.5}$): C, 53.04; H, 6.23; N, 9.28. Found: C, 53.16; H, 5.96; N, 9.44.

*[Cu^I(**L6**)(ClO$_4$)].* Ligand **L6** (40 mg, 0.14 mmol) was treated with an equimolar amount of $[Cu^I(CH_3CN)_4](ClO_4)$ (45 mg, 0.14 mmol) in acetone (3.0 mL) under N_2 atmosphere in a glovebox. After stirring the mixture for 10 min at ambient temperature, addition of ether (100 mL) to the mixture gave a white powder that was precipitated by standing the mixture for several minutes. The supernatant was then removed by decantation, and the remaining white solid was washed with ether several times and dried to give complex $[Cu^I(\mathbf{L6})(ClO_4)]$ in 62%. FT-IR (KBr) ν 1095 cm^{-1} (ClO_4^-); HRMS (FAB$^+$): m/z = 358.1348, calcd for $C_{19}H_{25}CuN_3$ 358.1344; Anal. Calcd for $[Cu^I(\mathbf{L6})(ClO_4)]\cdot 0.25H_2O$ ($C_{19}H_{25.5}CuClN_3O_{4.25}$): C, 49.30; H, 5.55; N, 9.08. Found: C, 49.06; H, 5.77; N, 9.18.

*[Cu^{II}(**L6**)(Cl)$_2$].* Ligand **L6** (20 mg, 68 μmol) was treated with an equimolar amount of $Cu^{II}Cl_2$ (9.1 mg, 68 μmol) in CH_3CN (3.0 mL). After stirring the mixture for 10 min at ambient temperature, addition of ether (100 mL) to the solution gave a green powder that was precipitated by standing the mixture for several minutes. The supernatant was then removed by decantation, and the remaining green solid was washed with ether three times and dried to give complex $[Cu^{II}(\mathbf{L6})(Cl)_2]$ in 48%. Single crystals of $[Cu^{II}(\mathbf{L6})(Cl)_2]$ were obtained by vapor diffusion of ether into a CH_3CN solution of the complex. HRMS (FAB$^+$): m/z = 393.1031, calcd for $C_{19}H_{25}ClCuN_3$ 393.1033; Anal. Calcd for $[Cu^{II}(\mathbf{L6})(Cl)_2]$ ($C_{19}H_{25}Cl_2CuN_3$): C, 53.09; H, 5.86; N, 9.77. Found: C, 53.08; H, 5.46; N, 9.81.

X-ray Structure Determination. All single crystals obtained in this study were mounted on a CryoLoop (Hamptom Research Co.) with mineral oil, and all X-ray data were collected on a Rigaku R-AXIS RAPID diffractometer using filtered Mo Kα radiation. The structures were solved by direct method (SIR2008) and expanded using Fourier techniques. Non-hydrogen atoms were refined anisotropically by full-matrix least-squares on F^2. Hydrogen atoms were attached at idealized positions on carbon atoms and were not refined. All structures in the final stages of refinement showed no movement in the atom positions. The calculations were performed using Single-Crystal Structure Analysis Software, version 3.8 (Rigaku Corporation: The Woodlands, TX, 2000−2006). Crystallographic parameters are summarized in Table 1. Atomic coordinates, thermal parameters, and intramolecular bond distances and angles are deposited in the Supporting Information (CIF file format).

Table 1. Summary of the X-ray Crystallographic Data of Copper(I) Complex $[Cu^I(L7)](PF_6)$, and Copper(II) Complexes $[Cu^{II}(L7)(Cl)_2]$ and $[Cu^{II}(L6)(Cl)_2]$

compound	$[Cu^I(\mathbf{L7})](PF_6)$	$[Cu^{II}(\mathbf{L7})(Cl)_2]$	$[Cu^{II}(\mathbf{L6})(Cl)_2]$
formula	$C_{20}H_{27}N_3CuPF_6$	$C_{20}H_{27}N_3CuCl_2$	$C_{38}H_{50}N_6Cu_2Cl_4$
formula weight	517.96	443.90	859.76
crystal system	monoclinic	triclinic	triclinic
space group	$P2_{1/n}$ (#14)	$P\bar{1}$ (#2)	$P\bar{1}$ (#2)
a, Å	16.6950(5)	7.4178(3)	11.4341(4)
b, Å	9.1363(2)	9.9823(4)	13.7012(6)
c, Å	15.1901(5)	14.4429(6)	14.2858(5)
α, deg	90.000	97.407(1)	103.335(2)
β, deg	109.9990(0)	91.232(1)	107.866(1)
γ, deg	90.000	103.157(1)	107.168(2)
V, Å^3	2177.2(1)	1031.24(7)	1904.0(2)
Z	4	2	2
F(000)	1064.00	482.00	892.00
D_{calcd}, g/cm^{-3}	1.580	1.487	1.500
T, K	103	103	103
crystal size, mm	0.20 × 0.20 × 0.10	0.50 × 0.30 × 0.20	0.30 × 0.20 × 0.10
(Mo Kα), cm^{-1}	11.399	13.331	14.343
$2\theta_{max}$, deg	55.0	54.9	55.0
no. of reflns meads	20804	10204	18704
no. of reflns obsd	4971	4681	8631
no. of variables	307	276	451
R^a	0.0352	0.0420	0.0451
$R_w{}^b$	0.0966	0.1387	0.1230
GOF	1.248	0.975	0.931

$^aR = \Sigma||F_0| - |F_c||/\Sigma|F_0|$. $^bR_w = [\Sigma(w(|F_0| - |F_c|)^2/\Sigma wF_o^2)]^{1/2}$.

Resonance Raman Spectroscopy. Resonance Raman scattering was excited at 442 nm from a He−Cd laser (Kimmon Koha, IK5651R-G) and 355 nm from an Nd:YAG laser (Photonic Solutions, SNV-20F), respectively. Resonance Raman scattering was dispersed by a single polychromator (Ritsu Oyo Kogaku, MC-100DG) and was detected by a liquid nitrogen cooled CCD detector (Horiba Jobin Yvon, Symphony CCD-1024 × 256-OPEN-1LS). The resonance Raman measurements were carried out using a rotating NMR tube (outer diameter = 5 mm) thermostated at −85 °C by flashing cold nitrogen gas. A 135° backscattering geometry was used.

Ligand Hydroxylation Reaction. Typically, $[Cu^I(\mathbf{L7})]^+$ (9.8 mg, 19 μmol) was dissolved into deaerated acetone (3.0 mL) under anaerobic conditions at ambient temperature, and then the solution was exposed to O_2 gas and stirred for 15 min at −85 °C. The alkoxide copper(II) complex in the final reaction mixture was detected by ESI-MS (pos.); m/z = 387.1883, calcd for $C_{20}H_{26}CuN_3O$ 387.1372. A mixture of **L7**−OH (hydroxylated ligand) and **L7** (original ligand) was obtained after an ordinary workup treatment of the reaction mixture with NH_4OH(aq) and following extraction by CH_2Cl_2. The yield **L7**−OH was determined as 30% based on the copper(I) starting material by comparing an integral ratio in the ^{1}H NMR spectrum between the

dx.doi.org/10.1021/ic501461n | Inorg. Chem. 2014, 53, 8786−8794

Scheme 2. Synthesis of Ligands L7 and L6

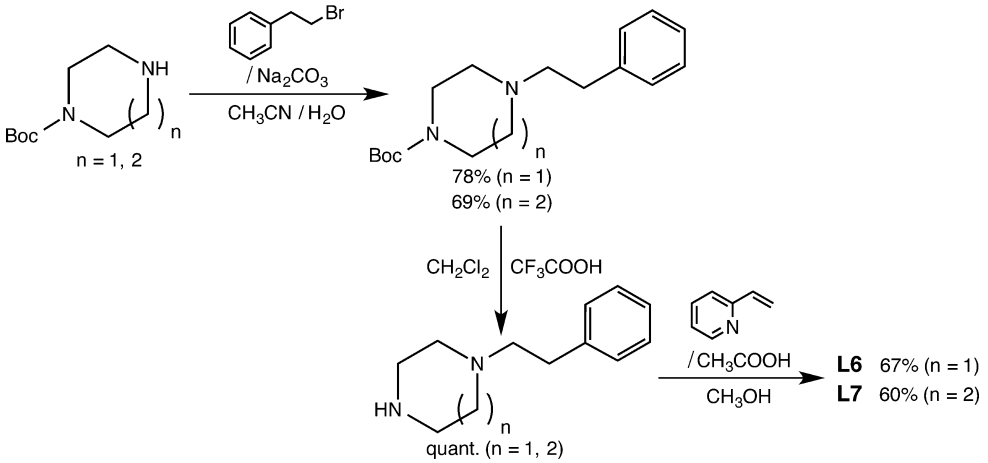

benzylic proton (−C*H*-OH−) at δ 4.63 (dd, J = 3.6 and 6.8 Hz) of **L7**−OH and the 6-position pyridine protons at δ 8.53 from both **L7**−OH and **L7**.

Kinetic Measurements. Kinetic measurements for the oxygenation reaction of the copper(I) complex $[Cu^{I}(\mathbf{L7})]^{+}$ were performed using a Hewlett-Packard 8453 photo diode array spectrophotometer with a Unisoku thermostated cryostat cell holder USP-203 (a desired temperature can be fixed within ±0.5 °C) in acetone at −85 °C. To start the oxygenation reaction of the copper(I) complexes, O_2 gas was rapidly introduced into a solution of the copper(I) complex in a UV cell (1.0 cm path length) through a silicon rubber cap by using a gastight syringe, and the increase of the absorption band due to the intermediates were monitored. Rate constants for the decomposition processes (k_{dec}) of the intermediates were monitored from the plots of ln(ΔA) vs time based on the time course of the absorption change at λ_{max} due to the intermediate.

RESULTS AND DISCUSSION

Synthesis of Ligands and Copper Complexes. The tridentate ligands involving seven-membered and six-membered cyclic diamine frameworks, **L7** and **L6**, were prepared according to the synthetic procedures outlined in Scheme 2. The reaction of monoprotected cyclic diamine with Boc group and (2-bromoethyl)benzene in the presence of Na_2CO_3 in CH_3CN/H_2O gave the corresponding phenethyl derivatives, which were then converted to the secondary amines by deprotection of the Boc group using CF_3COOH. Michael addition of the secondary amines to 2-vinylpyridine gave **L7** and **L6**, respectively.

Treatment of ligands **L7** and **L6** with $[Cu^{I}(CH_3CN)_4](PF_6)$ and $[Cu^{I}(CH_3CN)_4](ClO_4)$ in acetone under anaerobic conditions (in a glovebox) gave the corresponding copper(I) complexes, $[Cu^{I}(\mathbf{L7})](PF_6)$ and $[Cu^{I}(\mathbf{L6})(ClO_4)]$, respectively. The copper(II) chloride complexes, $[Cu^{II}(\mathbf{L7})(Cl)_2]$ and $[Cu^{II}(\mathbf{L6})(Cl)_2]$, were obtained by the reaction of ligands **L7** and **L6** with $Cu^{II}Cl_2$ in acetonitrile.

The ligand 1-(2-phenethyl)-5-[2-(2-pyridyl)ethyl]-1,5-diazacyclooctane (**L8**) and the corresponding copper(I) complex $[Cu^{I}(\mathbf{L8})](PF_6)$ and copper(II) chloride complex $[Cu^{II}(\mathbf{L8})(Cl)](PF_6)$ were synthesized according to the reported procedure.[19,20]

Copper(I)-O_2 Reactivity. As reported in our previous paper, copper(I) complex $[Cu^{I}(\mathbf{L8})]^{+}$ reacted with O_2 in acetone at a low temperature (−85 °C) to provide a mononuclear copper(II) end-on superoxide complex **S**, exhibiting characteristic absorption bands at 397 nm (ε = 4200 M^{-1} cm^{-1}), 570 nm (850), and 705 nm (1150) (dashed line in Figure 1).[19]

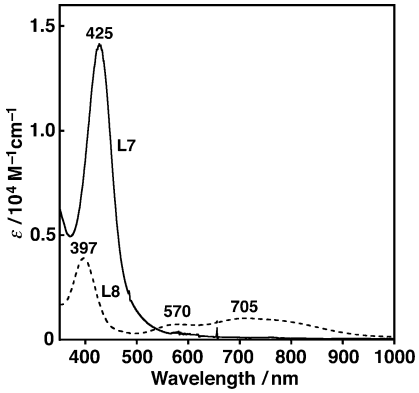

Figure 1. UV−vis spectra of **O** (solid line) and **S** (dashed line) generated by oxygenation of $[Cu^{I}(\mathbf{L7})]^{+}$ (0.20 mM) and $[Cu^{I}(\mathbf{L8})]^{+}$ (0.20 mM) in acetone at −85 °C, respectively.

Oxygenation reaction of the copper(I) complex of ligand **L7**, $[Cu^{I}(\mathbf{L7})]^{+}$, under the same experimental conditions gave a completely different spectrum having an intense absorption band at 425 nm (ε = 14 100 M^{-1} cm^{-1}) as shown in Figure 1 (solid line). The spectrum is nearly identical to those of the well-established bis(μ-oxido)dicopper(III) complexes,[5,6] indicating formation of a similar dicopper-dioxygen adduct **O** (Scheme 1). In support of this notion, stoichiometry of the oxygenation reaction was determined as Cu:O_2 = 2:1 by the Stack's method (titration of the oxygenated product with ferrocene monocarboxylic acid, see Figure S1).[24] Complex **O** readily decomposed even at the low temperature (lifetime ∼50 s at −85 °C) to induce a benzylic ligand hydroxylation of the phenethyl side arm, giving an alcohol product in a 34% yield (maximum yield 50%) based on the copper(I) starting complex after workup treatment (see Experimental Section and Figure S2). Rate-dependence on the reaction temperature (Eyring plot, see Figures S3 and S4) gave the activation parameters for the ligand hydroxylation process as $\Delta H^{\ddagger}$ = 35 ± 2.5 kJ mol^{-1} and $\Delta S^{\ddagger}$ = −92 ± 13 J K^{-1} mol^{-1}. These values are similar to those of the intramolecular aliphatic ligand hydroxylation reactions in the bis(μ-oxido)dicopper(III) complexes so far been reported in the literature.[5,25] Although instability of **O** hampered further characterization, the similarity in the UV−vis

dx.doi.org/10.1021/ic501461n | Inorg. Chem. 2014, 53, 8786−8794

spectrum as well as the reactivity strongly support the formation of the bis(μ-oxido)dicopper(III) complex **O** in the present system with ligand **L7**. It should be noted that the aliphatic hydroxylation reactivity of **O** is 10^3 times higher than that of **S** under the same experimental conditions (k_{dec} = 2.5 × 10^{-4} s^{-1} for **L8** and k_{dec} = 2.8 × 10^{-1} s^{-1} for **L7** at −60 °C, see Figure S2).[19,20]

The drastic difference in ligand hydroxylation reactions could be mainly attributed to the difference in the oxidizing ability of the respective copper-active oxygen complexes (**S** vs **O**).

In the case of ligand **L6**, no active-oxygen intermediate was detected during the course of the reaction of copper(I) complex and O_2 under the same conditions (at −85 °C in acetone), but a copper(II)-acetate complex $[Cu^{II}(\mathbf{L6})(OAc)]^+$ was generated even at the low temperature (Figure S5). The acetate ligand may be generated by a Bayer−Villiger type oxidation reaction of acetone (solvent) and subsequent hydrolysis of generated methyl acetate.[26] Consequently, subtle ligand modification (different ring size of cyclic diamine moiety) resulted in significant differences in copper(I)/O_2 reactivity (Scheme 3).[17,22,27−29] In order to get insight into the ligand effects, crystal structures of the copper(I) and copper(II) complexes of these ligands were carefully examined as described below.

Scheme 3. O_2-Reactivity of Copper(I) Complexes Supported by L8, L7, and L6

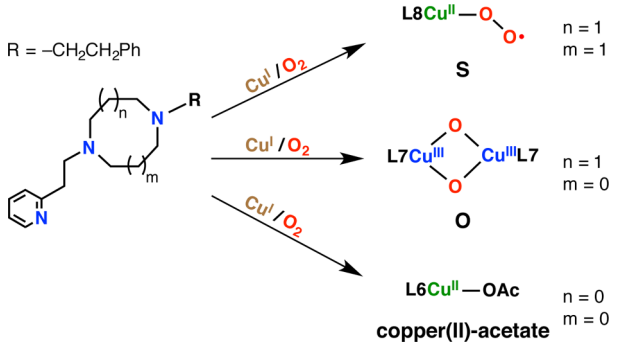

Crystal Structure of Copper(I) Complexes. The crystal structure of $[Cu^{I}(\mathbf{L7})]^+$ is shown in Figure 2A together with the crystallographic data summarized in Table 1. The crystal structure of $[Cu^{I}(\mathbf{L8})]^+$ was already reported in our previous reports,[19] and its expanded view around the copper(I) center is presented in Figure 2B together with that of $[Cu^{I}(\mathbf{L7})]^+$ in Figure 2C. In spite of our great efforts, however, treatment of **L6** with $[Cu^{I}(CH_3CN)_4](PF_6)$ only gave an oily material, and that with $[Cu^{I}(CH_3CN)_4](ClO_4)$ provided a white powder material. Thus, single crystals of copper(I) complex of **L6** suitable for X-ray crystallographic analysis have yet to be obtained.

The copper(I) complex $[Cu^{I}(\mathbf{L7})]^+$ exhibits a three-coordinate T-shape structure ligated by the three nitrogen atoms, N(1), N(2), and N(3), of the supporting ligand (Figure 2A,C), in which the copper(I) ion is in the trigonal plane consisting of three N atoms (deviation from the plane is only 0.0518(2) Å). Thus, the overall structure of $[Cu^{I}(\mathbf{L7})]^+$ is similar to that of the copper(I) complex $[Cu^{I}(\mathbf{L8})]^+$, which also exhibited a three-coordinate T-shape structure.[19] However, detailed inspection of the structures of the metal centers has pointed out a notable difference in the bond angle of N(2)−Cu(1)−N(3) at the diamine moiety. Namely, the reduction of the ring size of the cyclic diamine moiety from eight (in $[Cu^{I}(\mathbf{L8})]^+$) to seven (in $[Cu^{I}(\mathbf{L7})]^+$) resulted in decrease of the bond angle from 90.30° to 80.56°, although the bond angles of N(1)−Cu(1)−N(2) at the pyridylethylamine moiety are nearly identical as ca. 102° (see, Figure 2B,C). As a result, the bond angle of N(1)−Cu(1)−N(3) of $[Cu^{I}(\mathbf{L7})]^+$ (175.42°) becomes larger than that of $[Cu^{I}(\mathbf{L8})]^+$ (167.5°). In the case of ligand **L6** bearing the smallest six-membered cyclic diamine, the bond angle of the cyclic diamine moiety, N(2)−Cu(1)−N(3), might be further decreased, and thus that of N(1)−Cu(1)−N(3) might be increased, if such a three-coordinate copper(I) complex were formed. However, such a three-coordinate copper(I) complex having a larger bond angle of N(1)−Cu(1)−N(3) might not be so stable. This may be a reason why the three-coordinate copper(I) complex could not be obtained in the reaction of ligand **L6** and $[Cu^{I}(CH_3CN)_4](PF_6)$ (with noncoordinating counteranion PF_6^-) (vide ante). Thus, it is assumed that the copper(I) complex obtained using $[Cu^{I}(CH_3CN)_4](ClO_4)$ instead of $[Cu^{I}(CH_3CN)_4](PF_6)$ has a four-coordinate structure, in which the counteranion ClO_4^- may coordinate to the metal center to give $[Cu^{I}(\mathbf{L6})(ClO_4)]$ having a four-coordinate tetrahedral structure (see, Experimental Section). Such structural differences among the copper(I) complexes supported by **L8**, **L7**, and **L6** are reflected in the different reactivity as described below.

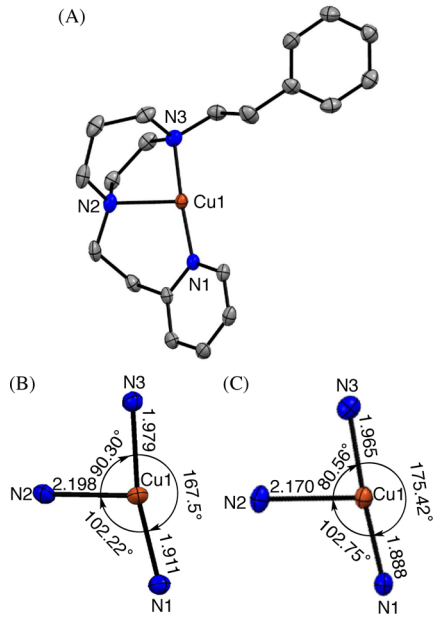

Figure 2. ORTEP drawings of (A) $[Cu^{I}(\mathbf{L7})]^+$ showing 50% probability thermal ellipsoids. The counteranion and hydrogen atoms are omitted for clarity. Expanded views of the core structures of (B) $[Cu^{I}(\mathbf{L8})]^+$ and (C) $[Cu^{I}(\mathbf{L7})]^+$. Interatomic distances of N(2)−N(3) are 2.964 and 2.678 Å for $[Cu^{I}(\mathbf{L8})]^+$ and $[Cu^{I}(\mathbf{L7})]^+$, respectively. The overall structure of $[Cu^{I}(\mathbf{L8})]^+$ was reported in the literature.[19]

Crystal Structures of Copper(II) Complexes. More prominent differences were found in the crystal structures of copper(II) complexes. The crystal structure of the copper(II) chloride complex $[Cu^{II}(\mathbf{L8})(Cl)]^+$ was reported in our previous papers, which exhibits a four-coordinate distorted tetrahedral geometry with the N_3Cl donor set (Figure 3C).[19,20] On the other hand, the copper(II) complexes $[Cu^{II}(\mathbf{L7})(Cl)_2]$ and $[Cu^{II}(\mathbf{L6})(Cl)_2]$ show five-coordinate distorted trigonal bipyr-

dx.doi.org/10.1021/ic501461n | Inorg. Chem. 2014, 53, 8786−8794

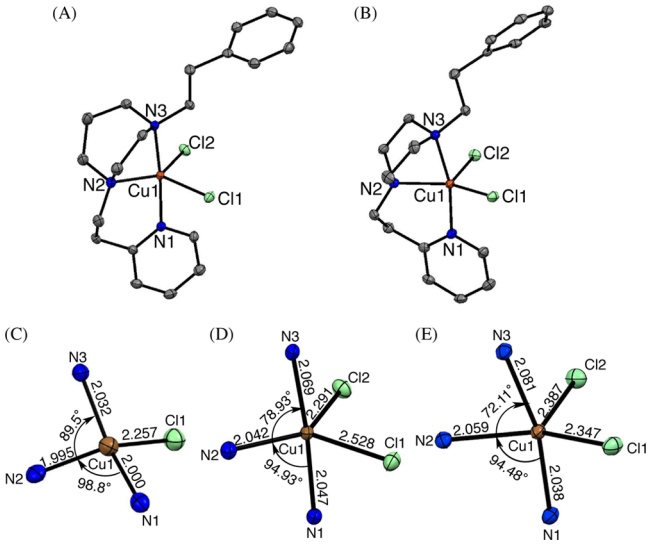

Figure 3. ORTEP drawings of (A) $[Cu^{II}(\mathbf{L7})(Cl)_2]$ and (B) $[Cu^{II}(\mathbf{L6})(Cl)_2]$ showing 50% probability thermal ellipsoids. The hydrogen atoms are omitted for clarity. Expanded views of the core structures of (C) $[Cu^{II}(\mathbf{L8})(Cl)]^+$, (D) $[Cu^{II}(\mathbf{L7})(Cl)_2]$, and (E) $[Cu^{II}(\mathbf{L6})(Cl)_2]$. Interatomic distances of N(2)−N(3) are 2.836, 2.613, and 2.437 Å for $[Cu^{II}(\mathbf{L8})(Cl)]^+$, $[Cu^{II}(\mathbf{L7})(Cl)_2]$, and $[Cu^{II}(\mathbf{L6})(Cl)_2]$, respectively. The overall structure of $[Cu^{II}(\mathbf{L8})(Cl)]^+$ was reported in the literature.[19]

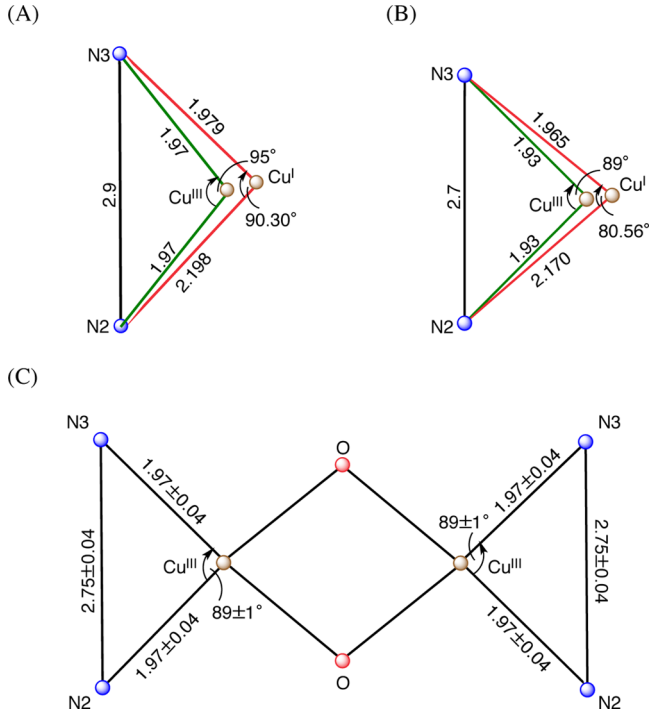

Figure 4. Presumed geometrical changes from the copper(I) complex (red line) to **O** (green line) in the (A) **L8** and (B) **L7** ligand systems. The crystal structural parameters of **O** reported in the literature.[30−32]

amidal geometry with the N_3Cl_2 donor set (Figure 3A, B, D, and E). As in the case of the copper(I) complexes (Figure 2), the bond angles of N(2)−Cu(1)−N(3) at the cyclic diamine moiety decrease in going from $[Cu^{II}(\mathbf{L8})(Cl)]^+$ (89.5°) to $[Cu^{II}(\mathbf{L7})(Cl)_2]$ (78.93°) to $[Cu^{II}(\mathbf{L6})(Cl)_2]$ (72.11°) (see, Figure 3C−E). The bond angle at the pyridylethylamine moiety N(1)−Cu(1)−N(2) of $[Cu^{II}(\mathbf{L8})(Cl)]^+$ (98.8°) is also larger than those of $[Cu^{II}(\mathbf{L7})(Cl)_2]$ (94.93°) and $[Cu^{II}(\mathbf{L6})(Cl)_2]$ (94.48°) (see, Figure 3C−E). As a result, $[Cu^{II}(\mathbf{L7})(Cl)_2]$ and $[Cu^{II}(\mathbf{L6})(Cl)_2]$ can provide enough space at the opposite site of N(2) to accommodate two chloride anions giving the five-coordinate structures, whereas $[Cu^{II}(\mathbf{L8})(Cl)]^+$ can accommodate only one chloride anion, providing the four-coordinate structure in the solid state. Since the steric bulkiness of the phenethyl and the pyridylethyl side arms is the same among the three ligands, the different structure of the copper complexes can be attributed to the geometric effect of the cyclic diamine moiety.

Geometric Effects of Cyclic Diamine Ligands (L8, L7, and L6). The geometry of the copper center might be an important factor in controlling the copper(I)/dioxygen reactivity. Inspection of the $(N_{eq})_2Cu(O)_2Cu(N_{eq})_2$ core structures (N_{eq} = equatorial nitrogen donor atom of N_2-bidentate and N_3-tridentate supporting ligands) of the reported bis(μ-oxido)dicopper(III) complexes **O** has revealed that the bite angle of N_{eq}−Cu−N_{eq} is 89 ± 1° and the Cu−N_{eq} and N_{eq}−N_{eq} interatomic distances are 1.97 ± 0.04 and 2.75 ± 0.04 Å, respectively (Figure 4C).[30−32]

In the case of copper(I) complex $[Cu^{I}(\mathbf{L7})]^+$, the bite angle of N(2)−Cu(1)−N(3) is 80.56° and the distance between N(2) and N(3) is 2.678 Å, which is close to that of **O** (2.75 ± 0.04 Å). Since the N(2)−N(3) distance is fixed around 2.7 Å regardless of the oxidation state of the copper ion (see figure captions of Figures 2 and 3) due to the rigidity of the cyclic diamine framework, enlargement of the bite angle of N(2)−Cu(1)−N(3) from 80.56° to 89° (ideal angle for **O**, see Figure 4C) enforces the bond lengths of Cu−N(2) (2.170 Å) and Cu−N(3) (1.965 Å) of the copper(I) complex of **L7** to be 1.93 Å according to the law of cosines (Figure 4B). This calculated (imaginary) bond length (1.93 Å) is very close to the Cu−N_{eq} bond lengths (1.97 ± 0.04 Å) required for the formation of the bis(μ-oxido)dicopper(III) complex **O** (Figure 4C). Therefore, it could be concluded that ligand **L7** is potentially suited to stabilize the bis(μ-oxido)dicopper(III) complex **O**.

In the case of $[Cu^{I}(\mathbf{L8})]^+$, on the other hand, the bite angle of N(2)−Cu(1)−N(3) is 90.30° in the copper(I) oxidation state (Figure 4A). This bite angle is very close to that of the bis(μ-oxido)dicopper(III) complexes (89 ± 1°) (Figure 2). In this case as well, the N(2)−N(3) distance is fixed around 2.9 Å regardless of the oxidation state of copper ion because of the rigidity of the cyclic diamine framework (see figure captions of Figures 2 and 3). Thus, in the case of **L8** ligand system, it would be difficult to reduce the Cu−N bond length from 2.198 to 1.97 Å, which is required for the formation of a bis(μ-oxido)dicopper(III) complex, since such a decrease in Cu−N bond length requires the much larger angle of N(2)−Cu(1)−N(3) as 95° (Figures 4A). In other words, ligand **L8** could not adapt to the nuclear arrangement required for the formation of the bis(μ-oxido)dicopper(III) complex from the copper(I) complex, but is better suited to a geometry of four-coordinate copper(II) complex as shown in Figure 3C. This may be an important reason why **L8** can stabilize the mononuclear copper(II)-superoxide complex.

In the **L6**-complex, the bite angle of N(2)−Cu(1)−N(3) (72.11°) and the interatomic distance of N(2)−N(3) (2.437 Å) are much smaller than those of **L8**- and **L7**-complexes (Figure 3). Due to the rigidity of the copper coordination geometry induced by the six-membered cyclic diamine moiety of **L6**, the ligand could stabilize neither the mononuclear nor the

dx.doi.org/10.1021/ic501461n | Inorg. Chem. 2014, 53, 8786−8794

dinuclear copper active oxygen species. Nonetheless, oxygenation of acetone (solvent molecule) took place upon the treatment of the copper(I) complex with O_2, suggesting formation of a certain type of reactive copper active-oxygen intermediate. Even though the starting material structure could not be determined, the active oxygen intermediate generated in the reaction of the copper(I) complex of **L6** and O_2 may induce Bayer–Villiger type oxidation of acetone to generate methyl acetate ($CH_3C(O)OCH_3$), which may be subsequently hydrolyzed to acetic acid, giving the copper(II)-acetate complex as experimentally detected (Figure S5).[26]

Ligand Effects on Redox Potential. Cyclic voltammograms of the copper(I) complexes have also demonstrated the ring size effect of cyclic diamine backbone. In Figure 5 are shown the cyclic voltammograms of the copper(I) complexes of **L6**, **L7**, and **L8** in acetone. Oxidation potential of the copper(I) complexes shifted toward the negative direction as the ring size of the cyclic diamine moiety decreased; $E_{1/2}$ = 0.40 V (**L8**), 0.18 V (**L7**), 0.12 V (**L6**) vs SCE. This clearly indicates that the smaller cyclic diamine ligand stabilizes the higher oxidation state of copper. Such a ligand effect might also be an important factor to control the copper(I)-O_2 reactivity. The reduction potential of the copper(II)-superoxide complex **S** supported by **L8** has already been reported as 0.19 ± 0.07 V vs SCE,[33] which is lower than the oxidation potential of copper(I) complex $[Cu^I(\mathbf{L8})]^+$ ($E_{1/2}$ = 0.40 V vs SCE) (Figure 5). Therefore, the reduction of **S** by $[Cu^I(\mathbf{L8})]^+$ is energetically disfavored, even though the bond-formation energy gained by the reaction between **S** and copper(I) is not clear. Thus, the mononuclear copper(II)-superoxide species **S** may be stabilized in the **L8** system. On the other hand, the oxidation potential of copper(I) complex $[Cu^I(\mathbf{L7})]^+$ is much lower at $E_{1/2}$ = 0.18 V vs SCE (Figure 5). Thus, $[Cu^I(\mathbf{L7})]^+$ might be easily oxidized by a mononuclear copper(II)-superoxide complex, if it is generated in situ, giving the bis(μ-oxido)dicopper(III) complex **O**. Oxidation potential of $[Cu^I(\mathbf{L6})(ClO_4)]$ is still lower ($E_{1/2}$ = 0.12 V vs SCE) as compared to that of $[Cu^I(\mathbf{L7})]^+$. Thus, the generated copper(II)-superoxide intermediate **S** or successively formed copper active-oxygen intermediate of **L6** may immediately oxidize acetone (solvent molecule) to give the acetate complex (Scheme 3).

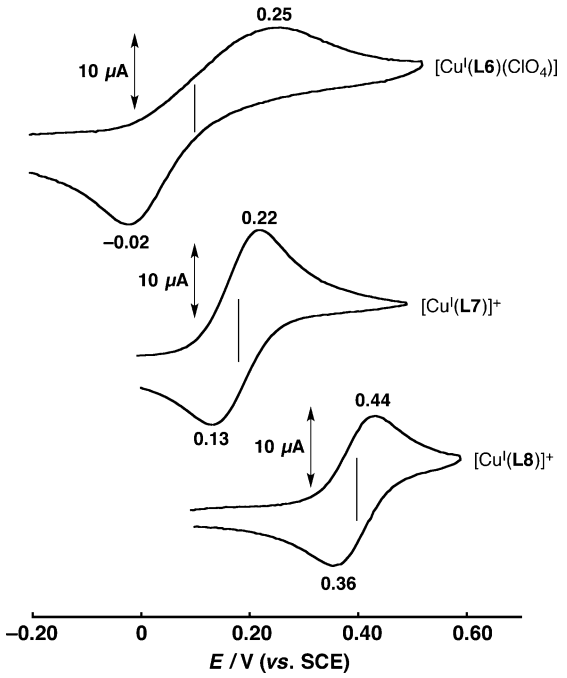

Figure 5. Cyclic voltammograms of $[Cu^I(\mathbf{L6})(ClO_4)]$, $[Cu^I(\mathbf{L7})]^+$, and $[Cu^I(\mathbf{L8})]^+$ (1.0 mM) in dry acetone containing $TBAPF_6$ (0.10 M) under N_2 atmosphere; working electrode glassy carbon, counter electrode Pt, reference electrode Ag/0.01 M $AgNO_3$. Scan rate is 50 mV/s.

Reactivity of Acyclic Diamine Ligand System. In order to evaluate the importance of rigidity of the cyclic diamine moiety of **L8**, **L7**, and **L6**, we have also examined the oxygenation reaction of the copper(I) complex supported by **LA** having a flexible acyclic propylene diamine framework (Chart 1). The synthetic procedures of **LA** and its copper(I) and copper(II) complexes are presented in the Supporting Information.

Figure 6A shows the spectral changes observed upon oxygenation of $[Cu^I(\mathbf{LA})]^+$ in acetone, where intense absorption bands at 358 and 396 nm readily appeared together with a weak band at 510 nm. Such absorption bands of the oxygenated products could be attributed to a (μ–η^2:η^2-peroxido)dicopper(II) complex ^{S}**P** and a bis(μ-oxido)dicopper(III) complex **O**, respectively (Scheme 4). Formation of these species was confirmed by the resonance Raman spectra shown in Figure 6B,C. When the reaction solution of $[Cu^I(\mathbf{LA})]^+$ with $^{16}O_2$ was excited with 355 nm laser light, an intense Raman band was observed 276 cm^{-1} that was not shifted upon $^{18}O_2$-substitution (Figure 6B). This peak was assigned to the Cu–Cu

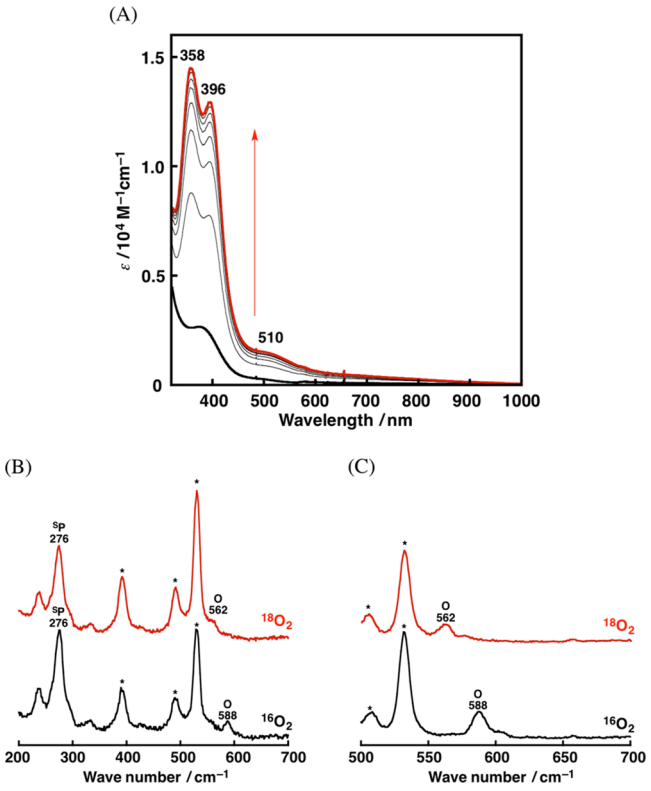

Figure 6. (A) UV–vis spectral change for the oxygenation of $[Cu^I(\mathbf{LA})]^+$ (0.20 mM) in acetone at −85 °C. Resonance Raman spectra of ^{S}**P** and **O** derived from the reaction of $[Cu^I(\mathbf{LA})]^+$ with $^{16}O_2$ (black curve) and $^{18}O_2$ (red curve) with (B) λ_{ex} = 355 nm and (C) λ_{ex} = 442 nm in acetone at −85 °C. Asterisks in the resonance Raman spectra denote solvent peaks.

dx.doi.org/10.1021/ic501461n | Inorg. Chem. 2014, 53, 8786–8794

Scheme 4. O_2-Reactivity of Copper(I) Complex Supported by LA

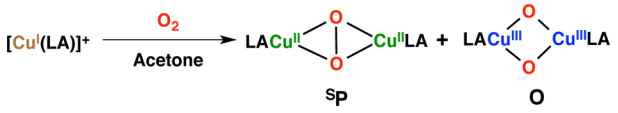

stretching vibration of the Cu_2O_2 core of (μ-η^2:η^2-peroxido)-dicopper(II) complex ^{S}**P**.[34] On the other hand, the Raman spectrum obtained by the excitation with 442 nm laser light gave a characteristic band at 588 cm^{-1}, which shifted to 562 cm^{-1} upon $^{18}O_2$-substitution (Figure 6C). The peak position at 588 cm^{-1} and its isotope shift of 26 cm^{-1} are within the range of those of the reported bis(μ-oxido)dicopper(III) complex **O** (Cu_2O_2 core breathing vibration involving Cu−O stretching).[35] In support of this notion, the stoichiometry of the oxygenation reaction was determined as Cu:O_2 = 2:1 by the titration of the oxygenated product with ferrocene monocarboxylic acid (Figure S6).

Ligand **LA** contains the N−CH_2−CH_2−CH_2−N unit in the molecular backbone as in the case of ligand **L8**. However, flexibility of the diamine moiety is significantly different between the two systems. Namely, the distance between the two nitrogen atoms in the acyclic diamine ligand **LA** system is largely altered depending on the oxidation state of copper ion (see Figure S7; N(2)−N(3): 3.298 Å in $[Cu^I(\mathbf{LA})]^+$ and 3.067 Å in $[Cu^{II}(\mathbf{LA})(Cl)]^+$), whereas that in the **L8**-complex is fixed around 2.9 Å regardless of the oxidation state of the copper ion (see figure captions of Figures 2 and 3). Thus, ligand **LA** can flexibly adapt to the structural changes required for the conversion of the copper(I) complex to the oxygenated products ^{S}**P** and **O** (Scheme 4). In other words, the O_2-copper(I) reactivity in the cyclic diamine ligand systems is strictly controlled by the rigidity of the chelate ring geometry. In accord with this notion, the acyclic ligand **LA** could not stabilize the mononuclear copper(II) superoxide complex, even though the copper(I) complex **LA**, $[Cu^I(\mathbf{LA})]^+$, has a similar oxidation potential (0.49 V vs SCE) to that of **L8**-complex (Figure S8), further demonstrating the importance of the rigid cyclic diamine moiety.

CONCLUSION

In summary, we have demonstrated that a subtle modification of the ring size of cyclic diamine moiety of the N_3-ligands resulted in a significant difference in copper(I)/dioxygen reactivity (Scheme 3). In the case of the copper(I) complex $[Cu^I(\mathbf{L8})]^+$, a copper(II)-superoxide complex **S** was solely generated, whereas a bis(μ-oxido)dicopper(III) complex **O** was formed in the case of $[Cu^I(\mathbf{L7})]^+$. On the other hand, however, no active-oxygen intermediate was detected in the reaction of $[Cu^I(\mathbf{L6})]^+$ with O_2. Such a significant difference in the O_2-reactivity of the copper(I) complexes could be attributed to the rigidity of the cyclic diamine moiety, which finely tunes the geometry as well as the electronic properties of the generated copper complexes. Detailed inspection of the copper(I) and copper(II) complexes have clearly indicated that the interatomic distance between the two nitrogen atoms of the cyclic diamine moiety is fixed regardless of the oxidation state of copper ion (Figures 2 and 3). That strictly defines the relation between the bond angle of N−Cu−N and the distance of N−Cu. Ligand **L7** can fit the structural change required for the formation of **O** from the copper(I) complex, since the N−N distance (2.678 Å) of the cyclic diamine moiety is nearly the same to that of **O** (Figure 4). Thus, reduction of the bond length of N−Cu (1.965 and 2.170 Å) in the copper(I) complex to 1.93 Å, which is required for the stabilization of high-valent copper(III) state of **O**, causes the increase of the bond angle of N−Cu−N from 80.56° to 89°, which is a ideal value for the formation of **O**. On the other hand, the N−N distance (~2.9 Å) in the **L8** system is larger than that of **O** (2.7 Å) (Figure 4), which might enforce the larger bite angle of N−Cu−N as 95°, if **O** was generated. Such a structural change might cause high molecular distortion, thus prohibiting the formation of the dicopper-dioxygen species. Notably, the ring size of the cyclic diamine moiety affects the redox potential of copper complex as shown in Figure 5. The observed O_2-reactivity is also consistent with the redox potentials of copper(I) complexes. Namely, the oxidation potential of $[Cu^I(\mathbf{L8})]^+$ (0.40 V vs SCE) is higher than the reduction potential of the superoxide complex **S** of **L8** (0.19 V vs SCE). Thus, further reaction of **S** and $[Cu^I(\mathbf{L8})]^+$ is energetically uphill, thus stabilizing the mononuclear copper-(II)-superoxide complex and prohibiting the formation of the dicopper active oxygen complexes such as **P** and **O**. On the other hand, the oxidation potential of $[Cu^I(\mathbf{L7})]^+$ is much lower than that of $[Cu^I(\mathbf{L8})]^+$, allowing it to react with a copper(II)-superoxide complex to give the dicopper complex **O**. This series of complexes and their reactivities are the first examples to validate entatic state theory in copper(I)/dioxygen chemistry with a series of ligands having subtle differences in the geometry of the donor atoms.[36] So far, steric bulkiness as well as the electron donor ability of the supporting ligands have been mainly considered to control the nuclearity in the copper(I)/dioxygen chemistry, but the present study has clearly demonstrated that the geometric effect of the supporting ligand is also important to control the reactivity of the copper(I) complexes toward dioxygen.

ASSOCIATED CONTENT

Supporting Information

Crystallographic data in CIF format. Further details are given in Figures S1−8 and Table S1−2. This material is available free of charge via the Internet at http://pubs.acs.org.

AUTHOR INFORMATION

Corresponding Author

*E-mail: shinobu@mls.eng.osaka-u.ac.jp.

Notes

The authors declare no competing financial interest.

ACKNOWLEDGMENTS

This work was supported by a Grant-in-Aid for Scientific Research on Innovative Areas “Molecular Activation Directed toward Straightforward Synthesis” (No. 22105007) and “Stimuli-responsive Chemical Species” (No. 24109015 and No. 25109540) and a Grant-in-Aid for Exploratory Research (No. 25620044) from the Ministry of Education, Culture, Sports, Science and Technology, Japan. Y.M. and S.I. express their special thanks to the JSPS Japanese-German Graduate Externship Program on “Environmentally Benign Bio- and Chemical Processes” for financial support of the stay in RWTH Aachen. T.A. is grateful for the financial support from Program for Leading Graduate Schools: “Interactive Materials Science Cadet Program”.

REFERENCES

(1) *Copper-Oxygen Chemistry*; Karlin, K. D., Itoh, S., Eds.; John Wiley & Sons, Inc.: Hoboken, NJ, 2011; Vol. *4*.
(2) Solomon, E. I.; Tuczek, F.; Root, D. E.; Brown, C. A. *Chem. Rev.* **1994**, *94*, 827−856.
(3) Solomon, E. I.; Sundaram, U. M.; Machonkin, T. E. *Chem. Rev.* **1996**, *96*, 2563−2606.
(4) Solomon, E. I.; Chen, P.; Metz, M.; Lee, S. K.; Palmer, A. E. *Angew. Chem., Int. Ed.* **2001**, *40*, 4570−4590.
(5) Lewis, E. A.; Tolman, W. B. *Chem. Rev.* **2004**, *104*, 1047−1076.
(6) Mirica, L. M.; Ottenwaelder, X.; Stack, T. D. P. *Chem. Rev.* **2004**, *104*, 1013−1045.
(7) Itoh, S. *Curr. Opin. Chem. Biol.* **2006**, *10*, 115−122.
(8) Wendlandt, A. E.; Suess, A. M.; Stahl, S. S. *Angew. Chem., Int. Ed.* **2011**, *50*, 11062−11087.
(9) Allen, S. E.; Walvoord, R. R.; Padilla-Salinas, R.; Kozlowski, M. C. *Chem. Rev.* **2013**, *113*, 6234−6458.
(10) Peterson, R. L.; Kim, S.; Karlin, K. D. In *Comprehensive Inorganic Chemistry II*; Reedijk, J. K. P., Ed.; Elsevier: Oxford, 2013; Vol. *3*, pp 149−177.
(11) Solomon, E. I.; Heppner, D. E.; Johnston, E. M.; Ginsbach, J. W.; Cirera, J.; Qayyum, M.; Kieber-Emmons, M. T.; Kjaergaard, C. H.; Hadt, R. G.; Tian, L. *Chem. Rev.* **2014**, *114*, 3659−3853.
(12) Itoh, S. In *Copper-Oxygen Chemistry*; Karlin, K. D., Itoh, S., Eds.; John Wiley & Sons: Hoboken, NJ, 2011; Vol. *4*, pp 225−282.
(13) Cramer, C. J.; Tolman, W. B. *Acc. Chem. Res.* **2007**, *40*, 601−608.
(14) Würtele, C.; Gaoutchenova, E.; Harms, K.; Holthausen, M. C.; Sundermeyer, J.; Schindler, S. *Angew. Chem., Int. Ed.* **2006**, *45*, 3867−3869.
(15) Kobayashi, Y.; Ohkubo, K.; Nomura, T.; Kubo, M.; Fujieda, N.; Sugimoto, H.; Fukuzumi, S.; Goto, K.; Ogura, T.; Itoh, S. *Eur. J. Inorg. Chem.* **2012**, *2012*, 4574−4578.
(16) Peterson, R. L.; Himes, R. A.; Kotani, H.; Suenobu, T.; Tian, L.; Siegler, M. A.; Solomon, E. I.; Fukuzumi, S.; Karlin, K. D. *J. Am. Chem. Soc.* **2011**, *133*, 1702−1705.
(17) Maiti, D.; Fry, H. C.; Woertink, J. S.; Vance, M. A.; Solomon, E. I.; Karlin, K. D. *J. Am. Chem. Soc.* **2007**, *129*, 264−265.
(18) Donoghue, P. J.; Gupta, A. K.; Boyce, D. W.; Cramer, C. J.; Tolman, W. B. *J. Am. Chem. Soc.* **2010**, *132*, 15869−15871.
(19) Kunishita, A.; Kubo, M.; Sugimoto, H.; Ogura, T.; Sato, K.; Takui, T.; Itoh, S. *J. Am. Chem. Soc.* **2009**, *131*, 2788−2789.
(20) Kunishita, A.; Ertem, M. Z.; Okubo, Y.; Tano, T.; Sugimoto, H.; Ohkubo, K.; Fujieda, N.; Fukuzumi, S.; Cramer, C. J.; Itoh, S. *Inorg. Chem.* **2012**, *51*, 9465−9480.
(21) Armarego, W. L. F.; Chai, C. L. L. *Purification of Laboratory Chemicals*, 6th ed.; Butterworth-Heinemann: Oxford, 2009.
(22) Mann, C. K.; Barnes, K. K. *Electrochemical Reactions in Non-aqueous Systems*; M. Dekker: New York, 1970
(23) Sellitto, G.; Faruolo, A.; de Caprariis, P.; Altamura, S.; Paonessa, G.; Ciliberto, G. *Bioorg. Med. Chem.* **2010**, *18*, 6143−6148.
(24) Herres-Pawlis, S.; Verma, P.; Haase, R.; Kang, P.; Lyons, C. T.; Wasinger, E. C.; Florke, U.; Henkel, G.; Stack, T. D. P. *J. Am. Chem. Soc.* **2009**, *131*, 1154−1169.
(25) Itoh, S.; Taki, M.; Nakao, H.; Holland, P. L.; Tolman, W. B.; Que, J. L.; Fukuzumi, S. *Angew. Chem., Int. Ed.* **2000**, *39*, 398−400.
(26) Kunishita, A.; Scanlon, J. D.; Ishimaru, H.; Honda, K.; Ogura, T.; Suzuki, M.; Cramer, C. J.; Itoh, S. *Inorg. Chem.* **2008**, *47*, 8222−8232.
(27) Tano, T.; Mieda, K.; Sugimoto, H.; Ogura, T.; Itoh, S. *Dalton Trans.* **2014**, *43*, 4871−4877.
(28) Tano, T.; Ertem, M. Z.; Yamaguchi, S.; Kunishita, A.; Sugimoto, H.; Fujieda, N.; Ogura, T.; Cramer, C. J.; Itoh, S. *Dalton Trans.* **2011**, *40*, 10326−10336.
(29) Itoh, S.; Fukuzumi, S. *Acc. Chem. Res.* **2007**, *40*, 592−600.
(30) Mahadevan, V.; Hou, Z.; Cole, A. P.; Root, D. E.; Lal, T. K.; Solomon, E. I.; Stack, T. D. P. *J. Am. Chem. Soc.* **1997**, *119*, 11996−11997.
(31) Mahapatra, S.; Halfen, J. A.; Wilkinson, E. C.; Pan, G.; Wang, X.; Young, V. G.; Cramer, C. J.; Que, L.; Tolman, W. B. *J. Am. Chem. Soc.* **1996**, *118*, 11555−11574.
(32) Mahapatra, S.; Young, V. G.; Kaderli, S.; Zuberbühler, A. D.; Tolman, W. B. *Angew. Chem., Int. Ed.* **1997**, *36*, 130−133.
(33) Tano, T.; Okubo, Y.; Kunishita, A.; Kubo, M.; Sugimoto, H.; Fujieda, N.; Ogura, T.; Itoh, S. *Inorg. Chem.* **2013**, *52*, 10431−10437.
(34) Henson, M. J.; Mahadevan, V.; Stack, T. D. P.; Solomon, E. I. *Inorg. Chem.* **2001**, *40*, 5068−5069.
(35) Holland, P. L.; Cramer, C. J.; Wilkinson, E. C.; Mahapatra, S.; Rodgers, K. R.; Itoh, S.; Taki, M.; Fukuzumi, S.; Que, L.; Tolman, W. B. *J. Am. Chem. Soc.* **2000**, *122*, 792−802.
(36) Vallee, B. L.; Williams, R. J. *Proc. Natl. Acad. Sci. U.S.A.* **1968**, *59*, 498−505.